

# Cytotoxicity assessment, inflammatory properties, and cellular uptake of Neutraplex lipid-based nanoparticles in THP-1 monocyte-derived macrophages

Nanobiomedicine

Volume 4: 1–14

© The Author(s) 2017

Reprints and permissions:

[sagepub.co.uk/journalsPermissions.nav](http://sagepub.co.uk/journalsPermissions.nav)

DOI: 10.1177/1849543517746259

[journals.sagepub.com/home/nab](http://journals.sagepub.com/home/nab)

Eric Berger<sup>1</sup>, Dalibor Breznan<sup>2</sup>, Sandra Stals<sup>1</sup>, Viraj J Jasinghe<sup>1</sup>, David Gonçalves<sup>3</sup>, Denis Girard<sup>3</sup>, Sylvie Faucher<sup>1</sup>, Renaud Vincent<sup>2</sup>, Alain R Thierry<sup>4</sup>, and Carole Lavigne<sup>1,3</sup>

## Abstract

Current antiretroviral drugs used to prevent or treat human immunodeficiency virus type 1 (HIV-1) infection are not able to eliminate the virus within tissues or cells where HIV establishes reservoirs. Hence, there is an urgent need to develop targeted delivery systems to enhance drug concentrations in these viral sanctuary sites. Macrophages are key players in HIV infection and contribute significantly to the cellular reservoirs of HIV because the virus can survive for prolonged periods in these cells. In the present work, we investigated the potential of the lipid-based Neutraplex nanosystem to deliver anti-HIV therapeutics in human macrophages using the human monocyte/macrophage cell line THP-1. Neutraplex nanoparticles as well as cationic and anionic Neutraplex nanolipoplexes (Neutraplex/small interfering RNA) were prepared and characterized by dynamic light scattering. Neutraplex nanoparticles showed low cytotoxicity in CellTiter-Blue reduction and lactate dehydrogenase release assays and were not found to have pro-inflammatory effects. In addition, confocal studies showed that the Neutraplex nanoparticles and nanolipoplexes are rapidly internalized into THP-1 macrophages and that they can escape the late endosome/lysosome compartment allowing the delivery of small interfering RNAs in the cytoplasm. Furthermore, HIV replication was inhibited in the *in vitro* TZM-bl infectivity assay when small interfering RNAs targeting CXCR4 co-receptor was delivered by Neutraplex nanoparticles compared to a random small interfering RNA sequence. This study demonstrates that the Neutraplex nanosystem has potential for further development as a delivery strategy to efficiently and safely enhance the transport of therapeutic molecules into human monocyte-derived macrophages in the aim of targeting HIV-1 in this cellular reservoir.

## Keywords

Nanomedicine, drug delivery nanosystem, siRNA, HIV, THP-1

Date received: 27 June 2017; accepted: 1 November 2017

<sup>1</sup> National Microbiology Laboratory, Public Health Agency of Canada, Winnipeg, Manitoba, Canada

<sup>2</sup> Inhalation Toxicology Laboratory, Environmental Health Science and Research Bureau, Health Canada, Ottawa, Ontario, Canada

<sup>3</sup> INRS-Institut Armand Frappier Centre, University of Quebec, Laval, Quebec, Canada

<sup>4</sup> Institute of Cancer Research of Montpellier, French National Institute of Health and Medical Research U986, Montpellier, France

## Corresponding author:

Carole Lavigne, National Microbiology Laboratory, JC Wilt Infectious Diseases Research Centre, 1015 Arlington Street, Winnipeg, Manitoba R3E 3R2, Canada.

Email [carole.lavigne@phac-aspc.gc.ca](mailto:carole.lavigne@phac-aspc.gc.ca)



Creative Commons Non Commercial CC BY-NC: This article is distributed under the terms of the Creative Commons Attribution-NonCommercial 4.0 License (<http://www.creativecommons.org/licenses/by-nc/4.0/>) which permits non-commercial use, reproduction and distribution of the work without further permission provided the original work is attributed as specified on the SAGE and Open Access pages (<https://us.sagepub.com/en-us/nam/open-access-at-sage>).

## Introduction

Since the discovery of HIV-1, the spread of the virus has grown from an epidemic to one of the world's most serious health challenges with approximately 37 million people living with the virus at the end of year 2016.<sup>1</sup> Highly active antiretroviral therapy (ART) allows the control of viral replication, delay or prevention of the progression to AIDS, increase of survival, and improvement of the quality of life of HIV-infected individuals. However, ART does not eliminate the virus. Hence, HIV is able to persist in the infected host even during prolonged ART.<sup>2,3</sup> Indeed, residual viremia is still detected in patients on ART when very sensitive methods are used<sup>4</sup> and HIV-1 reverts to measurable plasma level in less than 2 weeks when ART is interrupted.<sup>3,5,6</sup> It has been shown that HIV is able to establish reservoirs in anatomically sequestered sites such as the brain, gut, liver, and secondary lymphoid tissue where drug penetration is suboptimal, or within cells where the virus is latent, thus allowing reinfection and development of drug resistance.<sup>7–12</sup> Although resting CD4<sup>+</sup> T cells are known to be the main cellular reservoir for latent HIV-1 infection, cells belonging to the monocyte/macrophage lineage have been described as the most important reservoirs outside the bloodstream.<sup>13–15</sup> Findings suggest that in the presence of antiretroviral drugs, macrophages are likely the main source of plasma viremia.<sup>16,17</sup> In contrast to T cells, HIV infection in monocyte/macrophages is less cytopathic and renders them more resistant to apoptosis, thus extending their lifespan and making these cells a persistent reservoir of HIV regardless of the presence of ART.<sup>13,18,19</sup> Moreover, high expression of efflux transporters in monocyte/macrophages has been shown to contribute to the resistance of these cells to antiretroviral treatment.<sup>20,21</sup> Altogether HIV infection in macrophages may result in continued viral replication and the formation of HIV reservoirs. Therefore, the development of new strategies for eliminating or preventing viral replication in monocyte/macrophages is urgently needed to achieve viral eradication in HIV-1-infected patients.

One promising approach to enhance drug delivery and target HIV in reservoir sites is the use of nanomaterials.<sup>22–25</sup> We and others have shown the efficiency and benefits of using nanoformulations to deliver HIV therapeutics and target HIV in infected cells and reservoir sites including macrophages.<sup>26–31</sup> The aim of this study was to evaluate the potential of the Neutraplex (Nx) nanosystem to deliver therapeutic molecules in HIV reservoir sites using the THP-1 monocyte-derived macrophages (MDMs) as the *in vitro* cellular model. Cytotoxicity of Nx nanoparticles (NPs) was assessed on cell viability and membrane integrity of THP-1 MDMs. In addition, their inflammatory profile was determined by evaluating their effects on polymorphonuclear neutrophils (PMNs) apoptosis and on pro-inflammatory cytokine secretion in exposed THP-1 MDMs. Furthermore, their efficiency to deliver

anti-HIV therapeutics in human macrophages was evaluated by confocal microscopy studies in THP-1 MDMs using small interfering RNAs (siRNAs) complexed to Nx NPs (nanolipoplexes) as a proof-of-concept strategy. The unique properties of the Nx nanosystem are that it allows the production of nanolipoplexes NPs of opposite surface charges with similar size and great stability without changing the chemical composition, therefore the possibility to study the impact of surface charge on cellular uptake, internalization, and drug delivery. Here, two nanolipoplexes formulations with opposing surface net charge but similar size, Nx+12/siRNA (cationic) and Nx-40/siRNA (anionic), were prepared and compared for their capacity to be internalized into human macrophages and to deliver active siRNAs to block HIV replication using the *in vitro* TZM-bl infectivity assay.

## Materials and methods

### Materials

Diioctadecylamidoglycylspermine (DOGS) was purchased from PolyPeptide Laboratories (Strasbourg, France), dioleoylphosphatidylethanolamine (DOPE), fluorescein-labeled DOPE, and cardiolipin from Sigma-Aldrich (Oakville, Ontario, Canada). siRNAs and RNase-free water were purchased from Applied Biosystems (Foster City, California, USA). THP-1 monocyte/macrophage cell line was obtained from the American Type Culture Collection.<sup>32,33</sup> The human epithelial cancer cervical cell line TZM-bl was obtained through the US National Institutes of Health AIDS Research and Reference Reagent Program from Dr John C Kappes, Dr Xiaoyun Wu, and Tranzyme Inc (Durham, North Carolina, USA).<sup>34,35</sup> Roswell Park Memorial Institute (RPMI)-1640 and Dulbecco's minimum essential medium (DMEM) cell culture medium, phosphate-buffered saline (PBS), Hank's balanced salt solution (HBSS), phorbol myristate acetate (PMA), trypsin–ethylenediaminetetraacetic acid (EDTA) solution, dimethyl sulfoxide (DMSO), LysoTracker<sup>®</sup> Blue DND-2, and Texas Red<sup>®</sup> wheat germ agglutinin (WGA) were all purchased from Life Technologies (Burlington, Ontario, Canada). Cell-Titer-Blue<sup>®</sup> (CTB) Cell Viability, CytoTox-96<sup>®</sup> (lactate dehydrogenase (LDH)), and Beta-Glo<sup>®</sup> assay kits were obtained from Promega (Madison, Wisconsin, USA). Capture beads were purchased from Luminex (Austin, Texas, USA). Cytokine antibody pairs and standards were obtained from R & D Systems Inc. (Minneapolis, Minnesota, USA) (interleukines IL-1 $\beta$ , IL-8) and interleukins IL-6, IL-10, tumor necrosis factor alpha TNF- $\alpha$ , and streptavidin-phycoerythrin (streptavidin-PE) was obtained from Thermo Fisher Scientific, Waltham, Massachusetts, USA. Milli-Q and deionized water were produced by a Millipore water purification system (EMD Millipore, Etobicoke, Ontario, Canada). Analytical grade solvents and reagents were purchased from Sigma-Aldrich unless otherwise specified.

## siRNA

Synthetic double-stranded siRNA sequences were dissolved in sterile RNase-free water at a concentration of 50  $\mu$ M and stored as indicated by the manufacturer. SiRNAs used in this study include siCCR5 targeting C–C chemokine receptor type 5 (CCR5) labeled at the 3' end with Cy3 (sense strand: 5'-GGGCUCUAUUUUAUAGG-CUddt-3'), siCXCR4 targeting chemokine C–X–C motif receptor 4 (CXCR4; sense strand: 5'-GGAAGCUGUUGG-CUGAAAAdtd-3'), and a scrambled siRNA that bears no homology to the human genome which was used as a non-targeting random control siRNA (sense strand: 5'-AGUA-CUGCUUACGAUACGGdTdT-3').

## Preparation of lipidic NPs and nanolipoplexes

Nx lipid-based NPs were prepared as previously described.<sup>28</sup> Briefly, an ethanol solution of a lipid mixture containing 1-mg DOGS, 1-mg of DOPE, and 0.5-mg cardiolipin was injected in an aqueous solution to form small unilamellar vesicles (SUVs) with a final concentration of 6.25-mg/mL lipids. This preparation can be kept for over 9 months at 4°C.<sup>36</sup> To prepare fluorescein-labeled Nx (fluorescein isothiocyanate (FITC)-Nx) NPs, FITC-DOPE was used. Nanolipoplexes (Nx/siRNA) were prepared as previously described<sup>28</sup> by mixing the SUV suspension with siRNA in sterile RNase-free water at two different lipids: nucleic acid (NA) weight ratios to obtain cationic (Nx+12/siRNA) or anionic (Nx-40/siRNA) nanolipoplexes depending on the NA load charge in the formulation. After incubating for 30 min at room temperature, the mixture was slightly mixed and stored at 4°C until their use. Nanolipoplexes were used within 2 weeks from preparation.

## Particle size and surface charge

Particle size and zeta potential were measured by dynamic light scattering (DLS) using a Zetasizer Nano ZS (Malvern Instruments Limited, Worcestershire, UK) with 633-nm laser wavelength and a measurement angle of 173° (backscatter detection) at 25°C in water (pH 7.0). Zeta ( $\zeta$ ) potential was employed to evaluate surface charge density of the nanoformulations. The width of the DLS hydrodynamic diameter distributions is indicated by the polydispersity index. Nanoformulations were vortexed before analysis and each sample was measured in triplicate.

## Cell culture

The TZM-bl indicator cell line was generated from a clone of HeLa cells (JC.53, clone 13). TZM-bl cells express human CD4 and the human chemokine receptors CXCR4 and CCR5 and are highly sensitive to infection with diverse isolates of HIV-1. TZM-bl cells express  $\beta$ -galactosidase and luciferase under the control of HIV-1 promoter, which is transactivated by the Trans-Activator of Transcription (HIV-1 Tat) protein

in relation to the level of virus replication.<sup>34,35</sup> THP-1 cells were maintained in RPMI 1640 and TZM-bl cells in DMEM, supplemented with 10% heat-inactivated fetal bovine serum, 50- $\mu$ g/mL gentamicin, and 2-mM L-glutamine at 37°C, 5% carbon dioxide (CO<sub>2</sub>). THP-1 MDMs were obtained by adding PMA to the culture medium at a final concentration of 10 ng/mL. THP-1 cells were incubated for 3–5 days to allow the monocytes to differentiate into macrophages. MDMs will be referred to in the text and figures hereafter as macrophages. All cells were cultured in 75-cm<sup>2</sup> culture flasks at 37°C in a humidified atmosphere of 5% CO<sub>2</sub> and were harvested when they reached about 80–85% confluence using 0.25% trypsin-EDTA solution diluted in PBS.

## Cytotoxicity assays

**Exposure experiments.** THP-1 cells were seeded in flat-bottomed 96-well plates (Corning) at a density of  $2 \times 10^4$  cells per well and allowed to differentiate. Then macrophages were washed with PBS and 100  $\mu$ L of fresh complete culture medium containing different concentrations of nanoformulations was added to the cells. After the indicated time of exposure (2–48 h), cytotoxicity assays were performed as described below.

**Cell viability.** Cell viability was determined using the CTB Assay as per the manufacturer instructions. Various control wells were added to each plate: wells with culture medium only (background controls), wells with culture medium containing Nx (interference controls), cells without Nx (untreated controls), and cells + 10% DMSO (positive controls for cytotoxicity). After exposure to Nx, 20  $\mu$ L of CTB reagent was added to each well. Absorbance was measured by top reading at 560 nm using 590 nm as a reference wavelength using a BioTek Synergy Mx microplate spectrophotometer (Thermo Fisher Scientific, Nepean, Ontario, Canada). CTB reduction was calculated by absorbance at 2-h minus absorbance at 0 h to control for background absorbance. The percentage cell viability was obtained after normalizing the data by untreated control cells. Untreated cells served as 100% cell viability.

**LDH release.** The enzymatic activity of cytosolic LDH released extracellularly in the cell culture supernatants was measured using the CytoTox 96 nonradioactive colorimetric assay per the manufacturer instructions. After exposure to Nx nanoformulations, supernatants were collected and frozen at –80°C until their analysis for LDH activity; 50  $\mu$ L of supernatant of each sample was plated in 96-well plates and 50  $\mu$ L of substrate from the LDH assay kit was added to each well. The plate was then incubated for 30 min at room temperature in the dark. Absorbance was read at 490 nm using a BioTek Synergy Mx spectrophotometer. Culture medium control wells were used to correct for phenol red and endogenous LDH activity in the serum and untreated cells served to measure LDH spontaneously

released from cells. Cells treated with 10% DMSO served as positive controls. Data are reported as percentage release of LDH compared to untreated control cells.

### Pro-inflammatory assays

**Cytokine analysis.** THP-1 macrophages were exposed to Nx NPs for 48 h and cytokine secretion was measured in supernatants by a Luminex multiplex bead assay using an in-house developed panel for pro-inflammatory cytokines as described earlier.<sup>37</sup> Capture antibodies were linked to carboxylated beads and used for detection of cytokines (IL-1 $\beta$ , IL-6, IL-8, IL-10, and TNF- $\alpha$ ). Captured cytokines were measured using biotinylated-antibodies and streptavidin-PE. Beads were analyzed using a Luminex-100 instrument with data collection software version 1.7. Cytokine concentrations were determined from standard curves calculated using the curve fitting software MasterPlex QT v. 5.0.

**Neutrophil apoptosis assays.** Freshly isolated human PMNs from healthy donors were isolated by dextran sedimentation followed by centrifugation over Ficoll-Hypaque (Pharmacia Biotech Inc., Baie D'Urfé, Quebec, Canada) as previously described.<sup>38,39</sup> Blood donations were obtained from informed and consenting individuals according to institutionally approved procedures. Purity (> 98%) was verified by cytology from cytocentrifuged preparations stained with Diff-Quick staining (Fisher Scientific, Ottawa, Ontario, Canada). Cell viability was monitored by trypan blue exclusion before and after each treatment and was always  $\geq$  99%. PMNs were cultured in RPMI 1640 medium with 2 mM L-glutamine and 25 mM 4-(2-hydroxyethyl)-1-piperazineethanesulfonic acid with 100 units/mL penicillin and 50  $\mu$ g/mL streptomycin (Gibco™; Fisher Scientific, Ottawa, Ontario, Canada) supplemented with 10% heat-inactivated autologous serum at 37°C, 5% CO<sub>2</sub>, and  $10 \times 10^6$  cells/mL were treated with 100  $\mu$ g/mL of Nx or for 24 h. Control cultures were incubated with water (untreated control), 65 ng/mL granulocyte macrophage colony-stimulating factor (GM-CSF; PeproTech Inc., Rocky Hill, New Jersey, USA) (negative control), or 5  $\mu$ M arsenic trioxide (ATO; positive control) as previously described.<sup>39,40</sup> Neutrophil apoptosis was assessed by cytology as described earlier.<sup>38-40</sup> Cells were examined by light microscopy at 400 $\times$  final magnification and apoptotic neutrophils were defined as cells containing one or more characteristic, darkly stained pyknotic nuclei. Neutrophil spreading onto glass was assessed as previously described<sup>41</sup> by incubating  $5 \times 10^6$  cells/mL in RPMI 1640 supplemented with 1% autologous serum in 24-well plates at 37°C, 5% CO<sub>2</sub> in the presence of buffer (untreated control), 65 ng/mL GM-CSF (negative control),  $10^{-9}$  M formyl-methionyl-leucyl-phenylalanine (fMLP; positive control), or 100  $\mu$ g/mL of titanium dioxide (TiO<sub>2</sub>), Nx NPs for 12 h. After incubation, 10  $\mu$ L of the cell suspension were loaded onto a hemacytometer and further incubated

for 5 min at 37°C. Then immediately after incubation, cells were examined and counted based on their shape under a light microscope (Leica Microsystems Canada Inc., Richmond Hill, Ontario, Canada). Cells with irregular shape were recorded as spread and round cells as nonspread.

### Confocal studies

THP-1 cells were seeded in a glass flat-bottomed 96-well tissue culture plates for confocal microscopy (MatTek, Ashland, Massachusetts, USA) at a density of  $2 \times 10^4$  cells per well with culture medium containing PMA to allow differentiation. After 5 days of incubation, differentiated THP-1 cells were washed with PBS and fresh culture medium containing FITC-labeled Nx NPs at 4.4  $\mu$ g/mL or nanolipoplexes (Cy3-labeled anti-CCR5 siRNA complexed to nonfluorescent Nx NPs at a final concentration of 50 nM, corresponding to 8.8  $\mu$ g/mL NPs for Nx+12/Cy3-siCCR5 or 2.6  $\mu$ g/mL NPs for Nx-40/Cy3-siCCR5) was added to the wells. In control wells, only culture medium was added to the cells. Cells were incubated at 37°C for 30 min to 24 h, then washed with PBS and fresh culture medium without NPs was added to each well. Cellular uptake and internalization of FITC-Nx NPs or Nx/Cy3-siCCR5 nanolipoplexes were visualized using confocal laser scanning microscopy (LSM700; Carl Zeiss Canada, Toronto, Ontario, Canada). For localization studies, cells were stained for late endosomes/lysosomes using the blue fluorescent dye LysoTracker and for cellular membrane using the red fluorescent dye WGA as per the manufacturer protocols as described earlier.<sup>26</sup> Briefly, live cells were stained with 75 nM LysoTracker Blue DND-22 for 30 min prior to microscopy observation. For membrane staining, cells were fixed with cold methanol for 5 min at -20°C, then washed three times with 2-mL HBSS without phenol red and incubated with WGA conjugated with Texas Red for 10 min at room temperature.

### HIV inhibition assay

TZM-bl cells were seeded at  $6 \times 10^3$  cells per well in a 96-well microtiter plate and allowed to adhere overnight in a humidified CO<sub>2</sub> incubator at 37°C. Then, supernatants were removed and replaced by fresh complete DMEM culture medium containing various concentrations of cationic or anionic nanolipoplexes (Nx+12/ or Nx-40/siCXCR4 or Nx+12/ or Nx-40/random siRNA sequence) and cells were incubated for 24 h at 37°C. Following incubation, cells were rinsed to remove the nanolipoplexes suspension and were infected with HIV-1-IIIB at multiplicity of infection 0.1 for 2 h at 37°C. After infection, cells were rinsed to eliminate unbound viruses and fresh complete culture medium was added. Then, cells were incubated for an additional 24h at 37°C. After that time, HIV replication was evaluated by measuring  $\beta$ -galactosidase activity using the Beta-Glo assay accordingly to the manufacturer

**Table 1.** Physicochemical characterization of the lipoplexes used in this study.<sup>a</sup>

Lipoplexe	Ratio lipid-NA	Size (nm)	Polydispersity	Zeta potential (mV)
Nx only		83.4 ± 12.5	0.327 ± 0.035	+50.7 ± 2.0
Nx+12	13	92.2 ± 5.6	0.192 ± 0.016	+37.0 ± 5.5
Nx-40	3.9	93.5 ± 17.0	0.229 ± 0.043	-55.9 ± 3.3

Nx: Neutrplex; Nx+: cationic Nx lipoplexes; Nx-: anionic Nx lipoplexes; NA: nucleic acid.

<sup>a</sup>Particles mean diameter was measured by dynamic light scattering and surface charge by zeta potential. Nx lipoplexes were prepared as described in the Materials and methods using the control scrambled siRNA sequence. Values represent mean ± standard deviation of four different experiments ( $n = 4$ ).

instructions. Briefly, 100  $\mu$ L of Beta-Glo reagent was added to each well and plates were incubated for 30 min at room temperature. Light intensity of each well was measured using a BioTek Synergy 2 multimode instrument (Thermo Fisher Scientific, Nepean, Ontario, Canada). Various control wells were added to each plate: wells without cells (background controls), uninfected cells without nanolipoplexes (negative controls), infected cells without nanolipoplexes (positive controls), and infected cells treated with nanolipoplexes containing a nontargeting scrambled siRNA sequence (random controls).

### Statistics

Statistical analysis was performed using SigmaPlot (version 12.5). A  $p$  value of less than 0.05 was considered as statistically significant.

## Results

### Physicochemical characteristics of the nanoformulations

Particle size analysis and surface charge of Nx NPs and Nx/random siRNA nanolipoplexes were determined by DLS in water and summarized in Table 1. Small particles with a diameter under 100 nm were formed. The size of both the cationic Nx+12/random siRNA ( $92.2 \pm 5.6$  nm) and the anionic Nx-40/random siRNA ( $93.5 \pm 17$  nm) nanolipoplexes was slightly higher compared to Nx only NPs ( $83.4 \pm 12.5$  nm), indicating the presence of the siRNAs in the nanolipoplex formulations. Homogenous lipid NPs and nanolipoplexes were obtained with polydispersity varying from 0.192 to 0.327 depending on the nanoformulations (Table 1). Zeta potential varied depending on the ratio lipid: NA as expected being less positive when higher amount of NA was used in the preparation of the nanolipoplexes. Nx NPs containing no NA formed the highest positively charged particles ( $+50.7 \pm 2$  mV) while Nx+12 nanolipoplexes containing NA at a ratio of lipid: NA of 13 formed less positively charged particles ( $+37 \pm 5.5$  mV) and the Nx-40 nanolipoplexes containing the highest amount of NA with a lipid: NA ratio of 3.9 formed highly negatively charged particles ( $-55.9 \pm 3.3$  mV) compared to Nx NPs only. The DLS results indicated a narrow size distribution and a good colloidal stability of the NPs

(Online Supplementary Figure S1). The results were reproducible in multiple batches.

### Cytotoxicity assessment

First we evaluated the effects of the Nx NPs on THP-1 macrophages cell viability using the CTB assay and on cell integrity by measuring the amount of LDH released from the cells after 48 h of exposure to increased concentration of NPs from  $\mu$ g/mL 2.19 to 35  $\mu$ g/mL. As illustrated in Figure 1(a), Nx NPs did not affect macrophages cell viability or cytoplasmic membrane integrity up to 17.5  $\mu$ g/mL. When the cells were treated with 35  $\mu$ g/mL, cell viability decreased to 84.5% and release of LDH increased by 18% when compared to untreated control cells ( $p < 0.001$ ). Next, we wanted to investigate the effects of NPs on THP-1 macrophages cell viability and integrity over time (Figure 1(b)) looking at times earlier than 48 h to confirm we have not missed any possible transient cytotoxic effect that might have been observed within 24 h of exposure. Since we found that exposure to 35  $\mu$ g/mL of NPs for 48 h did not potentially affect the cells (Figure 1(a)), for this next series of experiments, we only used the two highest concentrations tested in the previous assay (17.5 and 35  $\mu$ g/mL) and added a higher concentration (70  $\mu$ g/mL) to further evaluate the cytotoxicity of the NPs (Figure 1(b)). We observed that the maximal effect on macrophages cell viability was already obtained after 4 h of incubation, 73 and 79% for 70 and 35  $\mu$ g/mL, respectively, but was not found statistically different from 48 h (for the 35  $\mu$ g/mL concentration; 84.5%, Figure 1(a)). The difference in cell viability over time was only found to be statistically significant at 35  $\mu$ g/mL between 4-h and 24-h post-incubation ( $p < 0.05$ ). The rate of CTB reduction within each time of incubation was not found to be concentration-dependent between 2 h and 24 h, although it was previously found statistically significant at 48 h (17.5 vs. 35  $\mu$ g/mL,  $p < 0.05$ ; Figure 1(a)). To note, NPs did not interfere with the CTB reduction assay as shown in Online Supplementary Figure S2. Maximum release of LDH (122%) was observed at 16 h in cells treated with 70  $\mu$ g/mL (Figure 1(c)) but was only found significantly higher when compared with cells incubated for 2 h (2 vs. 16h,  $p < 0.01$ ) and was not found to be statistically different from LDH release at 48 h (119%; data not shown). At 35  $\mu$ g/mL, LDH release was not found significantly higher at any time point between 2 h and 24 h than at

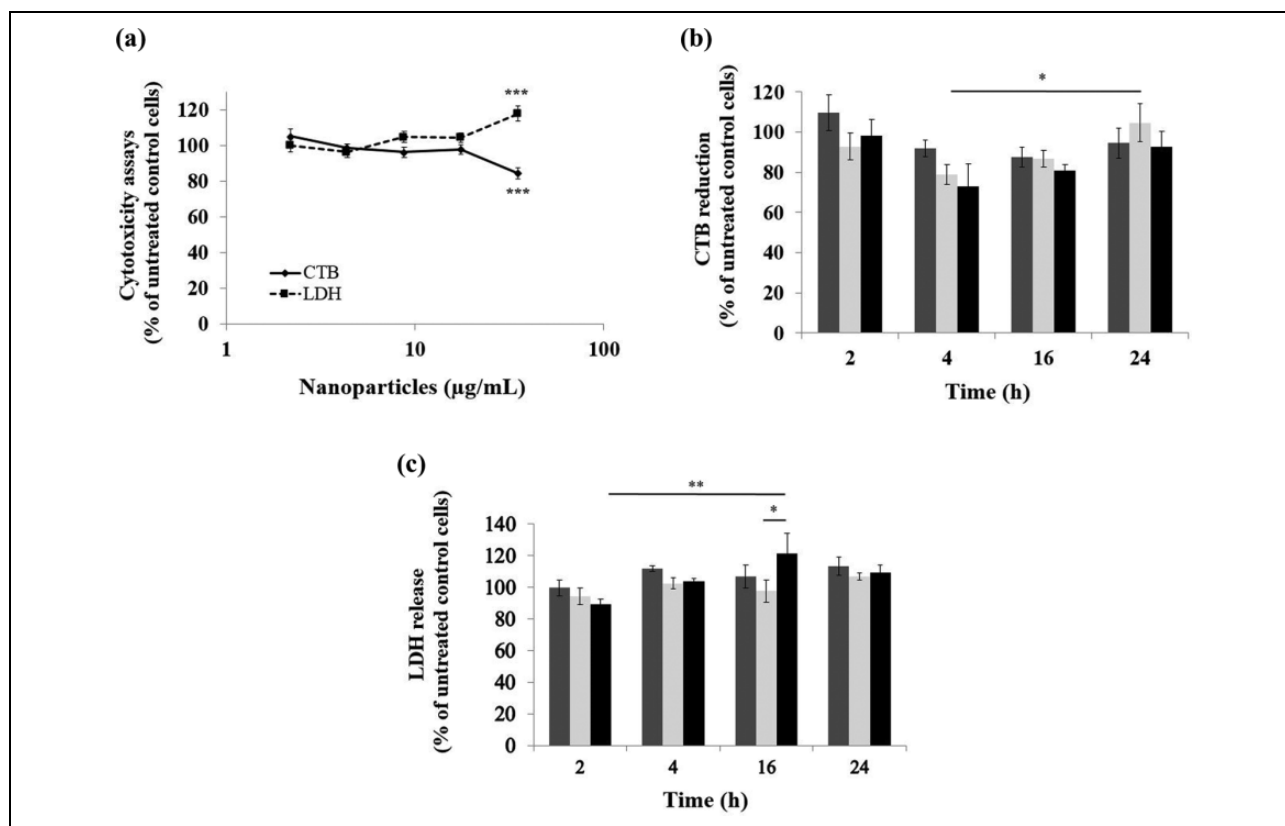


**Figure 1.** Cytotoxicity assays: Concentration-dependent effects and time-course of Nx nanoparticles. Macrophages were exposed to nanoparticles for A) 48h or B-C) the indicated time, then reduction of CellTiter-Blue and LDH release in culture supernatant were measured using the respective cytotoxicity assay as described in Materials and Methods. Data represent the means  $\pm$  SEM of A) three separate experiments done in triplicates or B-C) at least two independent experiments done in triplicates. B-C) Dark grey column: 17.5 µg/mL; Light grey column: 35 µg/mL; Black column: 70 µg/mL. Statistically significant based on a two-way ANOVA analysis A) Concentration, Assays or B-C) Concentration, Time. \* $p \leq 0.05$ ; \*\* $p \leq 0.01$ ; \*\*\* $p \leq 0.001$ .

48 h (118%; Figure 1(a)). A concentration-dependent effect on LDH release was only observed at 16-h post-incubation (Figure 1(c)) between 35 µg/mL and 70 µg/mL ( $p < 0.05$ ). At 48 h, we have also observed a significant difference between 17.5 µg/mL and 35 µg/mL ( $p < 0.05$ ; Figure 1(a)). THP-1 macrophages treated with 10% DMSO served as positive controls in these experiments and the results are shown in Online Supplementary Figure S3. At this concentration of DMSO, macrophages cell viability was already dramatically reduced at 2 h, while LDH release increased over time to be maximal at 24 h. These results validate the CTB and LDH assays performed.

### Cellular uptake and intracellular localization of NPs

Next, we wanted to evaluate the ability of human macrophages to internalize the Nx NPs. First, we performed a time course study by exposing THP-1 macrophage cells to 4.4 µg/mL of FITC-labeled Nx NPs for 30 min to 24 h. Uptake and localization of the FITC-Nx NPs were visualized using confocal microscopy and by staining the cells for late endosomes/lysosomes (LysoTracker Blue) and cellular membrane (WGA; Red) markers. Results of the time

course study are shown in Figure 3. After 30 min exposure, NPs were already found inside the cells (Figure 2(b)) and cell uptake increased over time significantly up to 24 h (Figure 2(b) and (d) to (f)). NPs seemed to be endocytosed by the macrophages since they were found to co-localize with the late endosome/lysosome marker at 30 min and 1.5 h (Figure 2(b) and (d), respectively). As early as 1.5-h post-exposure, fluorescent NPs showed a diffuse pattern in the cytoplasm of some cells indicating that they were able to escape the late endosomes/lysosomes compartment. After longer time of exposure (3 and 24 h), NPs were found mainly free in the cytoplasm of live cells (Figure 2(e) and (f), respectively). At the low concentration tested (4.4 µg/mL of NPs), after 24-h post-exposure, fluorescence in live cells was very bright and diffuse throughout the cytoplasm (Figure 2(f)). Next, we wanted to investigate whether the NPs could deliver siRNAs into macrophages. For these experiments, 50 nM Cy3-labeled siCCR5 (red fluorescence) was complexed with Nx NPs at two different lipids: NA ratios as described earlier and cellular uptake of nanolipoplexes was visualized 24 h after exposure in THP-1 macrophages stained for late endosomes/lysosomes (blue fluorescence). Results are shown in Figure 3. In

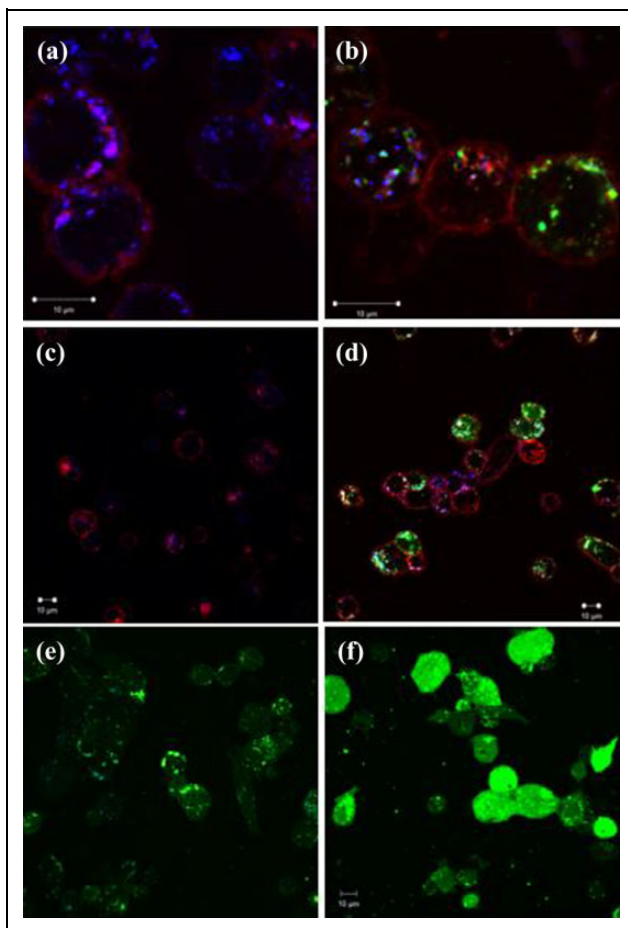


**Figure 2.** Time course of uptake and internalization of Nx nanoparticles in macrophages. Cells were exposed to FITC-labelled NPs (green fluorescence) for B) 30min, D) 1.5h, E) 3h, F) 24h at a final concentration of 4.4 $\mu$ g/mL. A and C) Untreated control cultures incubated without NPs for A) 30min or C) 1.5h. Cells were stained for A-E) late endosomes/lysosomes using Lysotracker (blue fluorescence) and A-D) cellular membrane using Wheat Germ Agglutinin (red fluorescence). E and F) Live cells. After incubation cells were washed and visualized by confocal microscopy. Multiple fields were analyzed and images are representative of two experiments.

control cells, no red fluorescence was observed (Figure 3(a) to (d)). In macrophages exposed to cationic nanolipoplexes Nx+12/Cy3-siCCR5 (Figure 3(e) to (h)), red fluorescence showed a punctate pattern and was found mainly inside the cells and not co-localized with late endosomes/lysosomes (Figure 3(g) and (h)). In some cells, fluorescent siRNAs were observed close to the cellular membrane still in a punctate pattern but not in the endosomal pathway and they were also found co-localized with the late endosomes/lysosomes marker. Anionic nanolipoplexes Nx-40/Cy3-siCCR5 were also efficiently taken up by macrophages (Figure 3(i) to (l)). At 24-h post-exposure, the red fluorescence showed also a punctate pattern but was not as bright as in the cells exposed to the cationic Nx+12/Cy3-siCCR5 nanolipoplexes (Figure 3(k) and (l)) and was found mainly

co-localized with the late endosomes/lysosomes marker (Figure 3(l)). However, when incubation was prolonged to 48 h, Cy3-siCCR5 uptake and delivery inside the cells was similar for both nanolipoplex formulations with very bright fluorescence mainly distributed throughout the cytoplasm and still showing a punctate pattern (Online Supplementary Figure S4). To note, cell morphology was not found different in control cultures than in cells exposed to either NPs alone or nanolipoplexes. Finally, Z-stacks analysis confirmed that the NPs were indeed internalized and not just adhering to the surface of the cells (data not shown).

### Pro-inflammatory effects of NPs

The pro-inflammatory effects of Nx NPs were investigated by first evaluating whether the NPs could alter neutrophil apoptosis rates measured by cytology and their ability to spread onto glass. As shown in Figure 4(a), after 24 h of culture, control neutrophils were approximately 40% apoptotic as measured by cytology. As expected, GM-CSF delayed apoptosis (22.5%), whereas ATO induced neutrophil apoptosis (70%). In this assay, Nx NPs were not found to modulate neutrophil apoptosis (46%) at the concentration tested (100  $\mu$ g/mL). To note, due to the limited number of donors (2–3 donors), these responses were not found to be statistically significant. In addition, because it was previously found that apoptotic neutrophils lose their ability to spread onto glass,<sup>42,43</sup> we investigated whether Nx NPs could regulate this response. The results shown in Figure 4(b) are in agreement with the cytology data showing that Nx NPs did not alter the neutrophil apoptotic rate. After 12 h of culture, the number of spread cells remained stable after exposure to 100- $\mu$ g/mL Nx NPs (25%) and was similar to the number of spread cells found in cells treated with water (17%). In contrast, cultures treated with GM-CSF, fMLP, or TiO<sub>2</sub> significantly increased the number of spread cells showing their ability to modify apoptotic rate in human neutrophils as we have previously reported.<sup>44,45</sup> Furthermore, Nx NPs were tested for their capacity to alter the production of pro-inflammatory cytokines by human macrophages using the THP-1 cell model. Since in the confocal studies we found that with only 4.4  $\mu$ g/mL, THP-1 cells were fully exposed to the Nx NPs, for this series of experiments we reasoned that exposure to the highest concentrations (35 and 70  $\mu$ g/mL) will not be necessary. We evaluated three concentrations (2.2, 8.8, and 17.5  $\mu$ g/mL). As illustrated in Figure 4(c), Nx NPs did not significantly induce pro-inflammatory cytokine secretion when compared to control cultures up to the highest concentration tested (17.5  $\mu$ g/mL).

### siRNA activity of nanolipoplexes

Next, we wanted to evaluate whether siRNAs complexed to Nx NPs could conserve their activity and be developed as anti-HIV therapeutics. To assess this, we used the TZM-bl

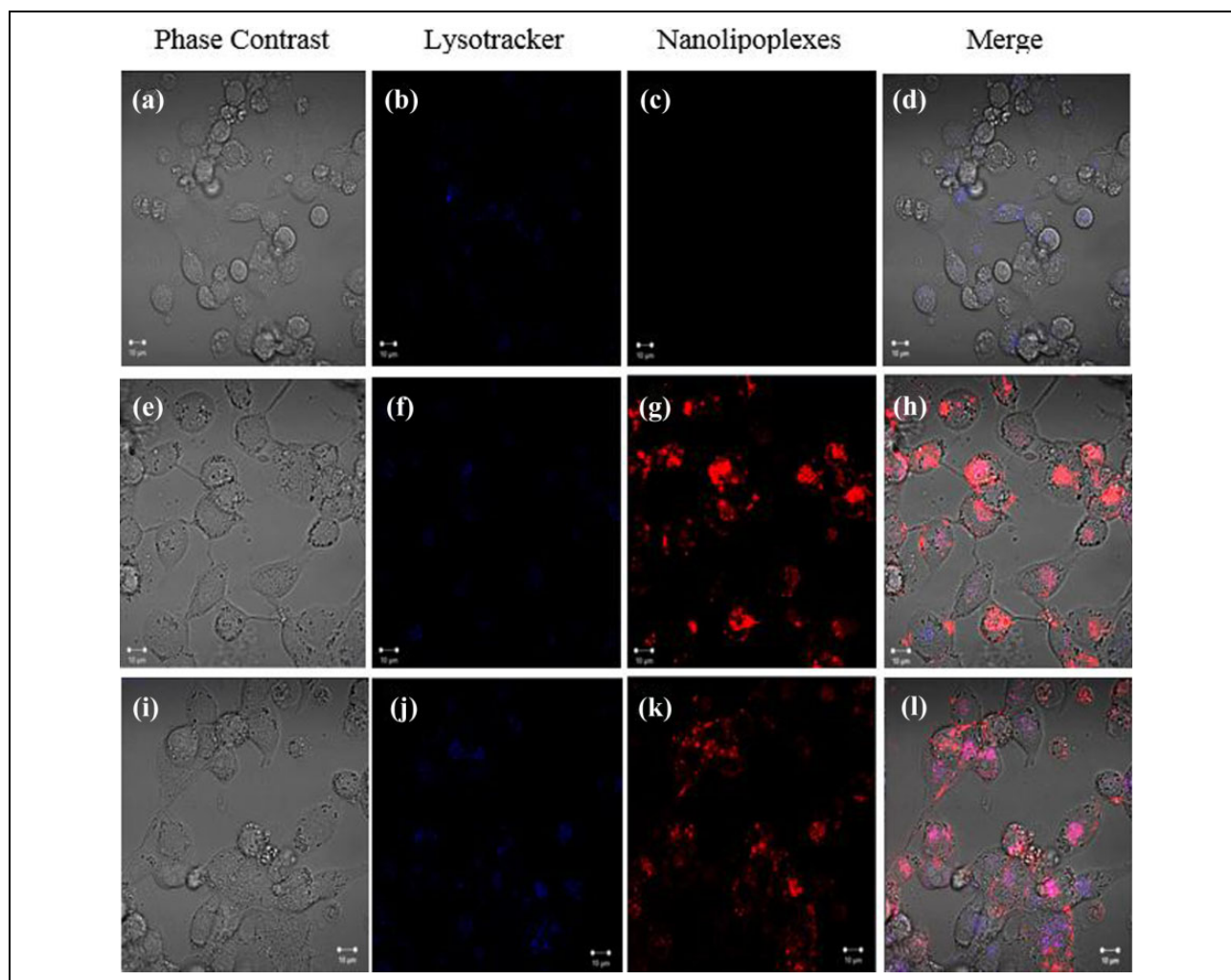


**Figure 3.** Uptake of nanolipoplexes in live macrophages. A-D) Untreated control cells incubated for 24h without nanolipoplexes, E-L) Cells exposed to nanolipoplexes (red fluorescence) at a final concentration of 50 nM for 24h: E-H) Nx+12/Cy3-siCCR5 (corresponding to 8.8  $\mu\text{g}/\text{mL}$  of NPs) or I-L) Nx-40/Cy3-siCCR5 (corresponding to 2.6  $\mu\text{g}/\text{mL}$  of NPs). After incubation cells were stained for late endosomes/lysosomes using Lysotracker (blue fluorescence), washed, and visualized by confocal microscopy. Multiple fields were analyzed and images are representative of two experiments.

reporter cell line which expresses CCR5, CXCR4, and CD4 molecules allowing the cells to be infected by HIV and previously validated anti-CXCR4 siRNAs for their RNAi activity.<sup>28</sup> First, we verified by confocal microscopy, the ability of the nanolipoplexes to be internalized by TZM-bl cells. We found that both nanolipoplexes were efficiently taken up by the cells and were able to escape the endosomes after 3 h of exposure (data not shown). Then, we performed the HIV inhibition assays. Data are shown in Figure 5 in terms of percent reduction of  $\beta$ -galactosidase activity compared to the nontargeting control siRNA sequence. In this assay, the highest level of inhibition of HIV replication observed was around 30% when using Nx-40/siCXCR4 nanolipoplexes at 12.5 and 25 nM when compared to Nx-40/random siRNA controls. However, although the results showed a concentration-dependent effect, it was not found statistically significant for both

nanolipoplex formulations at concentrations higher than 12.5 nM ( $p \leq 0.05$ ). Anionic Nx-40 nanolipoplexes showed higher inhibitory effect than cationic Nx+12 nanolipoplexes at all concentrations tested except at 100 nM, but again the differences were not found statistically significant. We also evaluated the effects of the Nx NPs alone (no siRNAs) on the replication of HIV-1 (Online Supplementary Figure S5). We found that at concentrations of NPs of 8.8  $\mu\text{g}/\text{mL}$  and higher,  $\beta$ -galactosidase activity was reduced when compared to untreated control cultures ( $p < 0.001$ ) indicating that the Nx NPs themselves can interfere with HIV-1 replication in this infectivity assay. In addition, the effect of Nx NPs alone on the viability of TZM-bl cells was evaluated using the CTB assay and no cytotoxicity was observed up to 35  $\mu\text{g}/\text{mL}$ , the highest concentration tested (Online Supplementary Figure S6). Finally, Nx/siRNA nanolipoplexes did not cause cytotoxicity in TZM-bl cells

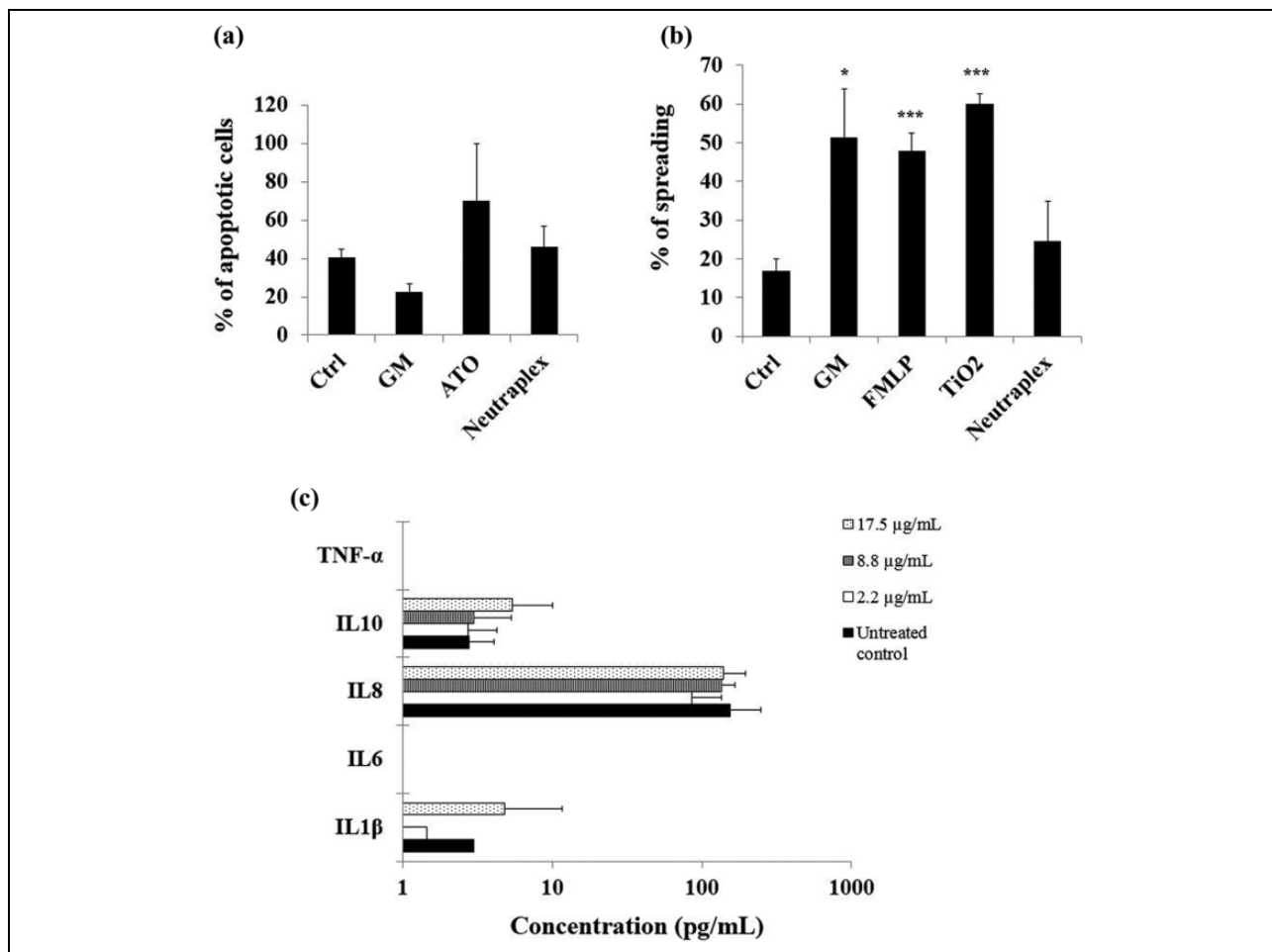


**Figure 4.** Inflammatory effects of Neutrplex nanoparticles. A) Effects on neutrophil apoptosis. Freshly isolated human polymorphonuclear cells (PMNs) ( $10 \times 10^6$  cells/mL) were incubated with water (Ctrl), 65ng/mL GM-CSF (GM), 5 $\mu$ M ATO, or 100 $\mu$ g/mL of Nx NPs for 24h, and apoptosis was assessed by cytology (Diff-Quick staining) as described in Materials and Methods. Results are means  $\pm$  SEM ( $n \geq 2$  different blood donors). B) Effects on neutrophil spreading. PMNs were incubated for 12h with water (Ctrl), 65ng/mL GM-CSF (GM),  $10^{-9}$ M fMLP, 100 $\mu$ g/mL TiO<sub>2</sub>, or 100 $\mu$ g/mL Nx NPs and the spreading of cells onto glass was assessed as described in Materials and Methods. Results are means  $\pm$  SEM ( $n=4$  different blood donors). C) Effects on cytokine secretion. THP-1 macrophages were exposed to increasing concentrations of Nx NPs for 48h then supernatants were collected. Concentration of cytokines present in the sample was analysed using a multiplex bead assay. Results are means  $\pm$  SD of duplicates. Data for IL-6 and TNF-alpha are below 1 pg/mL. \*,  $P < 0.05$  vs the control and \*\*\*,  $P < 0.001$  vs the control.

up to the highest concentration tested:  $111.05\% \pm 3.82\%$  and  $94.98\% \pm 5.01\%$  of untreated control cells with 200 nM of Nx+12/siRNA and 400 nM of Nx-40/siRNA, respectively (data not shown).

## Discussion

Macrophages are key players in HIV infection and contribute significantly to the cellular reservoirs of HIV. Hence, the virus can survive for prolonged periods in these cells despite ART (ART has been removed). Nanotechnology provides a means to overcome cellular and anatomical barriers to drug delivery and shows promises for its application in the area of HIV eradication and viral reservoir targeting.<sup>24,31</sup> In a previous study, Nx nanolipoplex formulations

were compared to the commercially available cationic Lipofectamine<sup>®</sup> RNAiMAX reagent (Thermo Fisher Scientific), for their cytotoxicity and capacity to deliver active siRNAs in HeLa-derived cells.<sup>28</sup> We have found that Nx NPs showed advantages over the commercial cationic RNAiMAX reagent in terms of stability, cytotoxicity, and cellular delivery. In addition, we reported for the first time the influence of surface charge on cytotoxicity and delivery properties of nanolipoplexes using the Nx nanosystem.<sup>28,46</sup> Here, we wanted to investigate the potential of the lipidic Nx nanosystem as a delivery strategy to target HIV reservoirs. Nx NPs and two nanolipoplex formulations (Nx+12/siRNA and Nx-40/siRNA) were prepared and characterized in terms of their size and surface charge. Physicochemical results obtained were similar to the findings of the previous

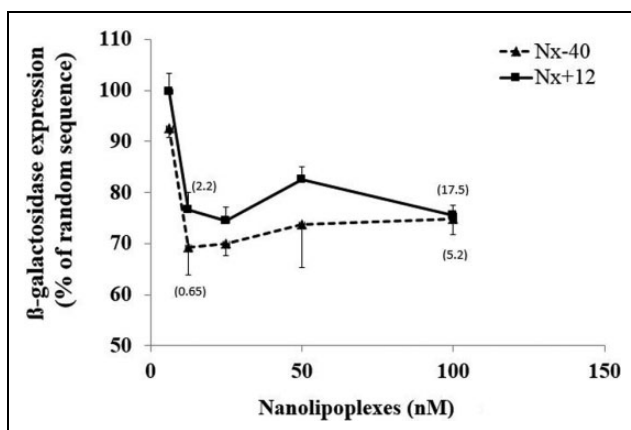


**Figure 5.** Inhibition of HIV-1 replication by Nx/siCXCR4 nanolipplexes. TZM-bl cells were first exposed to Nx nanolipplexes at the indicated concentration then cells were infected with HIV-1 for 2h at MOI 0.1. After 2h, fresh culture medium was added and cells were further incubated for 24h. HIV replication was monitored using the  $\beta$ -Glo assay as described in Materials and Methods. Data represent mean  $\pm$  SD of four replicates (for Nx-40/siCXCR4) or mean  $\pm$  SEM of two experiments with at least four replicates (for Nx+12/siCXCR4) and are corrected for background signal. Numbers in brackets represent the amount of lipid in  $\mu$ g/mL in the nanolipplex formulations.

study,<sup>28</sup> with stable and homogenous nanoformulations with sizes smaller than 100 nm and surface charges corresponding to the lipid: NA ratio. In addition, the Nx nanoformulations and NPs were stable at 4°C up to at least 1 and 9 months, respectively, in solution which represents a great advantage for future use in clinical application. Importantly, the nanoformulations did not aggregate in the presence of serum as per our microscopic observations (data not shown) allowing to perform experiments in biological conditions.

Macrophages obtained by differentiation of THP-1 monocytes were chosen as the *in vitro* cellular model<sup>32,33</sup> to assess cytotoxicity and pro-inflammatory effects of the Nx NPs, because it has been successfully used to investigate the toxicity of NPs on macrophages<sup>31,47–49</sup> and, in addition, they secrete macrophage-specific cytokines. First, cytotoxicity was assessed by two different bioassays (CTB reduction and LDH release), and time point experiments were performed to investigate time-dependent influence on the cytotoxic results. Here, we found that both cytotoxicity assays provided similar results in terms of the magnitude of the effect on the cells. Hence, Nx NPs did not seriously affect cell viability or membrane integrity of human macrophages since maximal effects observed were 27% decrease in cell viability and 22% increase in LDH release with the highest concentration evaluated (70  $\mu$ g/mL). Considering that it has been suggested that a decrease in cell viability by more than 30% is to be considered as a cytotoxic effect<sup>50</sup> and that high level of cellular uptake was observed with only 4.4  $\mu$ g/mL of Nx NPs, we can conclude that Nx NPs have a low cytotoxic profile for human macrophages.

Furthermore, our time point experiments revealed that the effect on enzymatic activity (CTB reduction) was observed more rapidly than the impact on cell integrity (LDH release) on cells exposed to the highest concentration (70  $\mu$ g/mL) of NPs, at 4 h compared to 16 h, respectively. This suggests that cellular enzymatic activity is more susceptible to the effect of Nx NPs, and impact on intracellular pathways might consequently lead to the cell membrane integrity damage observed later. We and others have previously reported a difference in sensitivity between cell viability and LDH release assays with nanomaterials. For instance, we found that the LDH release assay was more sensitive than the CTB reduction assay when evaluating carbon nanotubes, standard reference materials: silica and TiO<sub>2</sub> microparticles,<sup>51</sup> and with different size-fractionated particles collected in a small urban area in Canada.<sup>52</sup> In contrast, others have reported less sensitivity with the LDH release assay compared to the cell viability MTT assay when assessing cytotoxicity of solid lipid NPs.<sup>53,54</sup> Comparison between different nanotoxicity studies is difficult because they vary in terms of the choice of concentrations of nanomaterials, time of exposure, bioassays, and cell models. In addition to the bioassay, the nature and physicochemical characteristics of the nanomaterial itself influence the results of cytotoxicity assessment.<sup>55,56</sup>

Furthermore, it is well known that the cytotoxicity potential of a given compound varies with the cell type. In the present study, THP-1 macrophages were found to be more sensitive to Nx NPs than HeLa-derived epithelial cells as no CTB reduction was observed in TZM-bl cells treated with 35  $\mu$ g/mL of Nx NPs for 48 h. These findings are in line with previous studies which have also reported that macrophages were more responsive to nanomaterials than epithelial cells.<sup>51,52,57</sup> Furthermore, Nx NPs did not affect cell viability of neuronal cells in CTB assays up to the highest concentration evaluated, 70  $\mu$ g/mL (unpublished results). These findings indicate the potential of the Nx nanosystem for drug delivery in the central nervous system either to directly target HIV-1 in this sanctuary site including infected macrophages in the brain or via Nx-loaded monocytes that would migrate into the brain. Hence, we have previously shown the efficiency of the Nx nanosystem to deliver siRNAs in the brain of baboons showing their potential for *in vivo* application for neurodegenerative diseases and HIV-1 targeting in the central nervous system.<sup>58</sup> Others have reported using a murine model of neuroAIDS that *ex vivo* loaded MDMs with indinavir-encapsulated lipid NPs injected intravenously were able to target the brain and reduce HIV-1 replication in HIV-1 encephalitis brain regions.<sup>59</sup>

Effects of nanomaterials on cells not only depend on the initial concentration at the time of exposure but also to the actual amount of NPs taken up by a single cell.<sup>56</sup> Cellular uptake of a nanomaterial is mainly determined by its nanoscale size but also by its surface charge, shape, and its

composition.<sup>28,46,60,61</sup> In the current study, using live-cell confocal microscopy, we have investigated cellular uptake of Nx NPs by THP-1 macrophages, and we found that Nx NPs are rapidly taken up by the cells. Even though the exact mechanism of entry was not part of this study, we can speculate that they entered through an endocytic process since once internalized the Nx NPs were found in endosomal and lysosomal compartments. A transition into the endosomal pathway might represent an advantage for a delivery system aiming to target HIV in macrophages since it has been shown that the virus assembles in the endolysosomal compartments of macrophages.<sup>30,62</sup> Other entry mechanisms might also be involved such as temperature-independent uptake as we have previously reported in epithelial HeLa cells<sup>46</sup> or phagocytosis. Further studies are needed to confirm the exact uptake process of Nx NPs in THP-1 macrophages. Here, we observed that Nx NPs were able to rapidly escape the endosomal pathway as the NPs were found into the cytoplasm as soon as 1.5 h after exposure. Although the exact mechanism and kinetics of release of siRNAs has not yet been investigated, we can speculate based on previous studies that the presence of cardiolipin in Nx NPs might help to transition from lamellar to hexagonal ultrastructure and thus enhance lipid membrane fusion with endosomes allowing their content to leak into the cytosol (unpublished results<sup>63,64</sup>). Furthermore, siRNAs complexed to the NPs were found in the cytoplasm of macrophages in a nonhomogenous pattern outside the endosomal/lysosomal vesicles but never inside the nucleus demonstrating the efficiency of the Nx nanosystem to deliver siRNAs to their site of action. Indeed, we and others have previously reported and suggested that siRNAs localize in cytosol and to regions in close proximity to the nuclear membrane in a nonhomogenous pattern near RISC components creating a focal point for RNAi factories.<sup>65-68</sup> Our data indicating that siRNAs delivered by Nx NPs can localize in cytosol are in consonance with the previous studies and demonstrate the protective effect of Nx. Furthermore, the fact that Nx NPs localized in cytosol in a homogenous diffuse pattern while siRNAs harbored a more punctate distribution supports the breakdown of the nanolipoplex and delivery of siRNA for RNAi. However, although silencing activity of the siRNAs delivered by Nx NPs has been confirmed in the TZM-bl reporter cell model, silencing activity still need to be confirmed in macrophages and further investigation is ongoing. Interestingly, anionic nanolipoplexes were also efficiently taken up by the cells and able to escape the endosomes/lysosomes compartment but they stayed longer in this compartment compared to the cationic Nx nanolipoplexes suggesting that anionic Nx nanoformulations might be favorable for endosomal targeting. In addition, delivery of siRNAs could also be achieved with high level of efficiency using anionic Nx nanolipoplexes and siRNAs were found in the cells for up to 96 h, the last time point examined (data not shown). Considering that anionic nanolipoplexes contain less lipids for the same

amount of NAs than their cationic counterparts thus suggesting potentially less cytotoxicity, therefore, anionic nanoformulations represent an advantage for in vivo application. Furthermore, we and others have previously shown that anionic NPs achieved more widespread dispersal in the brains of rats and baboons than cationic NPs<sup>58,69,70</sup> showing their potential for brain delivery. Also, the fact that the intracellular uptake of the Nx nanoformulations was not affected by serum make them suitable for therapeutic application. Experiments are ongoing to further examine the interaction of the anionic and cationic nanolipoplexes with biological fluids such as blood and serum and to better investigate the possibility of their distinct mechanisms of uptake. Finally, in contrast to several NPs which have been found to exert pro-inflammatory properties such as zinc oxide (ZnO) or TiO<sub>2</sub>,<sup>44,71,72</sup> Nx NPs were not found to modulate neutrophil apoptosis or enhance the production of pro-inflammatory cytokines by THP-1 macrophage cells and were comparable to polylactide-co-glycolide (PLGA) NPs known for their low pro-inflammatory profile.<sup>31</sup> These findings are promising but warrant further in vivo immunotoxicological studies to clearly establish the immunomodulatory effect of Nx NPs and confirm their low inflammatory profile. Clearly, THP-1 is a valid and useful model for peripheral blood mononuclear cells (PBMCs).<sup>73</sup> However, it has also been shown that THP-1 cells produce less IL-6, IL-8, and IL-10 than PBMCs while showing a robust TNF- $\alpha$  production upon stimulation with lipopolysaccharides (LPS).<sup>74</sup> Here, we report that THP-1 cells produced no detectable amount of TNF- $\alpha$  and IL-6 and did not increase IL-8 and IL-1 $\beta$  level in response to Nx NPs. It is interesting to note that Nx NPs do not induce IL-8 production in THP-1 cells, indicating the absence of endotoxins in the NP preparations as endotoxins are known to be potent inducers of IL-8. Furthermore, although not found to be statistically significant, Nx NPs slightly induced IL-10 production at the highest dose tested, which is anti-inflammatory. This contrasts with our previous results showing the pro-inflammatory profile of secreted cytokines in THP-1 cells in response to silica particles (personal communication) or silver NPs<sup>75</sup> exposure. Altogether, these observations suggest that Nx NPs are not potent inducers of cytokine production in THP-1 cells. It should be interesting to verify the low inflammatory potential of Nx NPs using PBMCs from a panel of subjects, which should give insight into interindividual variability in Nx NPs reactivity. Further studies are needed to further characterize the inflammatory profile of Nx NPs.

Our results demonstrate the potential of Nx nanosystem to deliver active silencing siRNA targeting CXCR4 co-receptor. In a previous study, we have shown that siCXCR4 when delivered with cationic or anionic Nx nanolipoplexes downregulated CXCR4 in HeLa-derived cells; however, anionic nanoformulations showed less potency despite their high cellular uptake.<sup>28</sup> However, the impact of the downregulation of CXCR4 on the ability of HIV to replicate was

not evaluated. In the present study, using the same anti-CXCR4 siRNAs, cationic and anionic Nx nanolipoplexes were assessed for their ability to inhibit HIV replication in the HeLa-derived TZM-bl in vitro HIV inhibition assay. We found similar level of HIV inhibition with both nanolipoplexes containing siCXCR4 when compared to nanolipoplexes containing a random siRNA with a half-maximal inhibitory concentration (IC<sub>50</sub>) in the range of 40 nM. It is worth mentioning that Nx anionic nanolipoplexes showed silencing activity at lipid concentrations less than 1 µg/mL with a concentration of 12.5 nM siRNA, showing great potential for their therapeutic application considering their low cytotoxicity (>200 nM for Nx+12/siRNA and >400 nM for Nx-40/siRNA) and inflammatory profiles as cited above. Interestingly, the Nx nanosystem itself also showed HIV inhibitory effect in this model at concentrations equivalent and above 8.8 µg/mL. This anti-HIV activity might potentially be due to an interaction with Nx NPs with the virus particles inside the cells preventing them to complete their replication cycle. This anti-HIV property might be exploited as well in vivo to prevent HIV transmission and deserve further investigation. Also, by varying the siRNA sequence used in the nanoformulations, Nx nanolipoplexes could be designed to target any genes and diseases including those involved in viral latency. Furthermore, Nx nanosystem can be designed to deliver a combination of different siRNA sequences, allowing a multi-drug approach.<sup>76</sup> Finally, further HIV inhibitory experiments using HIV-infected MDMs are ongoing to confirm the potential of the Nx nanosystem to target HIV in this cellular reservoir.

## Conclusion

Nx NPs were prepared and evaluated for their potential to efficiently and safely deliver siRNA in cellular models. Cationic and anionic siRNA nanolipoplexes were proved to be efficient to protect and deliver NAs into the cytoplasm of macrophages with negligible toxicity and immunogenicity for the cells. Furthermore, both nanolipoplexes showed anti-HIV activity in a cell indicator assay. Although further investigation in vivo is required, altogether, these results demonstrate that the Nx nanosystem is a promising strategy to deliver therapeutic agents in human MDMs and could be used to target pathogens that proliferate inside macrophages including HIV-1, visceral leishmaniasis, malaria, and tuberculosis.

## Author contributions

Carole Lavigne is the principal investigator of this study. She designed the study, analyzed and interpreted the data, and wrote the manuscript. Dalibor Breznán and Renaud Vincent contributed to the design of the cytotoxicity assessment and the analysis and interpretation of the data and critically revised the manuscript. Denis Girard and Sylvie Faucher contributed to the design, analysis, and interpretation of the data for the inflammatory

experiments and critically reviewed the manuscript. Eric Berger, Sandra Stals, Viraj J Jasinghe, and David Gonçalves contributed to the acquisition and analysis of data and reviewed the manuscript for its final approval. Alain R Thierry contributed to the conception and design of the study and reviewed the manuscript.

## Declaration of Conflicting Interests

The author(s) declared no potential conflicts of interest with respect to the research, authorship, and/or publication of this article.

## Funding

The author(s) disclosed receipt of the following financial support for the research, authorship, and/or publication of this article: This work was supported by the Public Health Agency of Canada. Denis Girard was supported by the Institut de recherche Robert-Sauvé en santé et en sécurité du travail (grant 2010-0021).

## Supplementary material

Supplementary material for this article is available online.

## References

- UNAIDS, Global Report (2017) [http://www.unaids.org/sites/default/files/media\\_asset/20170720\\_Data\\_book\\_2017\\_en.pdf](http://www.unaids.org/sites/default/files/media_asset/20170720_Data_book_2017_en.pdf) (accessed 24 November 2017).
- Wong JK, Hezareh M, Gunthard HF, et al. Recovery of replication-competent HIV despite prolonged suppression of plasma viremia. *Science* 1997; 278: 1291–1295.
- Davey RT Jr, Bhat N, Yoder C, et al. HIV-1 and T cell dynamics after interruption of highly active antiretroviral therapy (HAART) in patients with a history of sustained viral suppression. *Proc Natl Acad Sci USA* 1999; 96: 15109–15114.
- Dornadula G, Zhang H, VanUitert B, et al. Residual HIV-1 RNA in blood plasma of patients taking suppressive highly active antiretroviral therapy. *JAMA* 1999; 282: 1627–1632.
- Harrigan PR, Whaley M, and Montaner JSG. Rate of HIV-1 RNA rebound upon stopping antiretroviral therapy. *AIDS* 1999; 13: F59–F62.
- Richman DD, Margolis DM, Delaney M, et al. The challenge of finding a cure for HIV infection. *Science* 2009; 323: 1304–1307.
- Chun TW, Nickle DC, Justement JS, et al. Persistence of HIV in gut-associated lymphoid tissue despite long-term antiretroviral therapy. *J Infect Dis* 2008; 197: 714–20.
- Palmer S, Josefsson L, and Coffin JM. HIV reservoirs and the possibility of a cure for HIV infection. *J Intern Med* 2011; 270: 550–560.
- Chun TW and Fauci AS. HIV reservoirs: pathogenesis and obstacles to viral eradication and cure. *AIDS* 2012; 26: 1261–1268.
- Peluso MJ, Ferretti F, Peterson J, et al. Cerebrospinal fluid HIV escape associated with progressive neurologic dysfunction in patients on antiretroviral therapy with well controlled plasma viral load. *AIDS* 2012; 26: 1765–1774.

11. Chan CN, Dietrich I, Hosie MJ, et al. Recent developments in human immunodeficiency virus-1 latency research. *J Gen Virol* 2013; 94: 917–932.
12. Van Lint C, Bouchat S, and Marcello A. HIV-1 transcription and latency: an update. *Retrovirology* 2013; 10: 67.
13. Gavegnano C and Schinazi RF. Antiretroviral therapy in macrophages: implication for HIV eradication. *Antivir Chem Chemother* 2009; 20: 63–78.
14. Kumar A, Abbas W, and Herbein G. HIV-1 latency in monocytes/macrophages. *Viruses* 2014; 6: 1837–1860.
15. Abbas W, Tariq M, Iqbal M, et al. Eradication of HIV-1 from the macrophage reservoir: an uncertain goal? *Viruses* 2015; 7: 1578–1598.
16. Crowe S, Zhu T, and Muller WA. The contribution of monocyte infection and trafficking to viral persistence, and maintenance of the viral reservoir in HIV infection. *J Leukoc Biol* 2003; 74: 635–641.
17. Stevenson M. Role of myeloid cells in HIV-1-host interplay. *J Neurovirol* 2015; 21: 242–248.
18. Montaner LJ, Crowe SM, Aquaro S, et al. Advances in macrophage and dendritic cell biology in HIV-1 infection stress key understudied areas in infection, pathogenesis, and analysis of viral reservoirs. *J Leukoc Biol* 2006; 80: 961–964.
19. Eisele E and Siliciano RF. Redefining the Viral Reservoirs That Prevent HIV-1 Eradication. *Immunity* 2012; 37: 377–388.
20. Jorajuria S, Dereuddre-Bosquet N, Becher F, et al. ATP binding cassette multidrug transporters limit the anti-HIV activity of zidovudine and indinavir in infected human macrophages. *Antivir Ther* 2004; 9: 519–528.
21. Robillard KR, Chan GN, Zhang G, et al. Role of P-glycoprotein in the distribution of the HIV protease inhibitor atazanavir in the brain and male genital tract. *Antimicrob Agents Chemother* 2014; 58: 1713–1722.
22. Vyas TK, Shah L, and Amiji MM. Nanoparticle drug carriers for delivery of HIV/AIDS therapy to viral reservoir sites. *Expert Opin Drug Deliv* 2006; 3: 613–628.
23. das Neves J, Amiji MM, Bahia MF, et al. Nanotechnology-based systems for the treatment and prevention of HIV/AIDS. *Adv Drug Deliver Rev* 2010; 62: 458–477.
24. Mallipeddi R and Rohan LC. Progress in antiretroviral drug delivery using nanotechnology. *Int J Nanomedicine* 2010; 5: 533–547.
25. Edagwa BJ, Guo D, Puligujja P, et al. Long-acting antituberculous therapeutic nanoparticles target macrophage endosomes. *The FASEB J* 2014; 28: 5071–5082.
26. Kell AJ, Slater K, Barnes ML, et al. Functionalized silica nanoparticles stable in serum-containing medium efficiently deliver siRNA targeting HIV-1 co-receptor CXCR4 in mammalian cells. *Int J Nano and Biomaterials* 2012; 4: 223–242.
27. Mahajan SD, Aslinkeel R, Law WC, et al. Anti-HIV-1 nanotherapeutics: promises and challenges for the future. *Int J Nanomedicine* 2012; 7: 5301–5314.
28. Lavigne C, Slater K, Gajanayaka N, et al. Influence of lipoplex surface charge on siRNA delivery: application to the in vitro downregulation of CXCR4 HIV-1 co-receptor. *Expert Opin Biol Ther* 2013; 13: 973–985.
29. Shibata A, McMullen E, Pham A, et al. Polymeric nanoparticles containing combination antiretroviral drugs for HIV type 1 treatment. *AIDS Res Hum Retroviruses* 2013; 29: 746–754.
30. Guo D, Zhang G, Wysocki TA, et al. Endosomal trafficking of nanoformulated antiretroviral therapy facilitates drug particle carriage and HIV clearance. *J Virol* 2014; 88: 9504–9513.
31. Guedj AS, Kell AJ, Barnes M, et al. Preparation, characterization, and safety evaluation of poly(lactide-co-glycolide) nanoparticles for protein delivery into macrophages. *Int J Nanomedicine* 2015; 10: 1–15.
32. Tsuchiya S, Yamabe M, Yamaguchi Y, et al. Establishment and characterization of a human acute monocytic leukemia cell line (THP-1). *Int J Cancer* 1980; 26: 171–176.
33. Tsuchiya S, Kobayashi Y, Goto Y, et al. Induction of maturation in cultured human monocytic leukemia cells by a phorbol diester. *Cancer Res* 1982; 42: 1530–1536.
34. Derdeyn CA, Decker JM, Sfakianos JN, et al. Sensitivity of human immunodeficiency virus type 1 to the fusion inhibitor T-20 is modulated by coreceptor specificity defined by the V3 loop of gp120. *J Virol* 2000; 74: 8358–8367.
35. Kappes JC and Wu X. Cell-based method and assay for measuring the infectivity and drug sensitivity of immunodeficiency virus. Patent 6,797,462 B1, USA, 2004.
36. Thierry AR, Abes S, Resina S, et al. Comparison of basic peptides- and lipid-based strategies for the delivery of splice correcting oligonucleotides. *Biochim Biophys Acta* 2006; 1758: 364–374.
37. Faucher S, Crawley AM, Decker W, et al. Development of a quantitative bead capture assay for soluble IL-7 receptor a in human plasma. *PLoS One* 2009; 4: e66.
38. Pelletier M, Bouchard A, and Girard D. In vivo and in vitro roles of IL-21 in inflammation. *J Immunol* 2004; 173: 7521–30.
39. Binet F, Cavalli H, Moisan E, et al. Arsenic trioxide (AT) is a novel human neutrophil pro-apoptotic agent: effects of catalase on AT-induced apoptosis, degradation of cytoskeletal proteins and de novo protein synthesis. *Br J Haematol* 2006; 132: 349–358.
40. Binet F and Girard D. Novel human neutrophil agonist properties of arsenic trioxide: involvement of p38 mitogen-activated protein kinase and/or c-jun NH2-terminal MAPK but not extracellular signal-regulated kinases-1/2. *J Leukoc Biol* 2008; 84: 1613–1622.
41. Pelletier M, Roberge CJ, Gauthier M, et al. Activation of human neutrophils in vitro and dieldrin-induced neutrophilic inflammation in vivo. *J Leukoc Biol* 2001; 70: 367–373.
42. Lee A, Whyte MK, and Haslett C. Inhibition of apoptosis and prolongation of neutrophil functional longevity by inflammatory mediators. *J Leukoc Biol* 1993; 54: 283–288.
43. Whyte MK, Meagher LC, MacDermot J, et al. Impairment of function in aging neutrophils is associated with apoptosis. *J Immunol* 1993; 150: 5124–5134.
44. Gonçalves DM, Chiasson S, and Girard D. Activation of human neutrophils by titanium dioxide (TiO<sub>2</sub>) nanoparticles. *Toxicol In Vitro* 2010; 24: 1002–1008.

45. Antoine F, Simard JC, and Girard D. Curcumin inhibits agent-induced human neutrophil functions in vitro and lipopolysaccharide-induced neutrophilic infiltration in vivo. *Int Immunopharmacol* 2013; 17: 1101–1107.
46. Resina S, Prevot P, and Thierry AR. Physico-chemical characteristics of lipoplexes influence cell uptake mechanisms and transfection efficacy. *PLoS One* 2009; 26: e6058
47. Chellat F, Grandjean-Laquerriere A, Naour RL, et al. Metalloproteinase and cytokine production by THP-1 macrophages following exposure to chitosan-DNA nanoparticles. *Biomaterials* 2005; 26: 961–970.
48. Chen HW, Su SF, Chien CT, et al. Titanium dioxide nanoparticles induce emphysema-like lung injury in mice. *FASEB J* 2006; 20: 2393–2395.
49. Grabowski N, Hillaireau H, Vergnaud J, et al. Surface coating mediates the toxicity of polymeric nanoparticles towards human-like macrophages. *Int J Pharmaceut* 2015; 482: 75–83.
50. International Organization for Standardization, ISO 10993-5: 2009. Biological Evaluation of Medical Devices Part 5: Tests for in Vitro Cytotoxicity. <https://www.iso.org/standard/36406.html>.
51. Kumarathasan P, Breznan D, Das D, et al. Cytotoxicity of carbon nanotube variants: a comparative in vitro exposure study with A549 epithelial and J774 macrophage cells. *Nanotoxicology* 2015; 2: 148–161.
52. Thomson EM, Breznan D, Karthikeyan S, et al. Cytotoxic and inflammatory potential of size-fractionated particulate matter collected repeatedly within a small urban area. *Part Fibre Toxicol* 2015; 12: 24.
53. Olbrich C, Bakowsky U, Lehr CM, et al. Cationic solid-lipid nanoparticles can efficiently bind and transfect plasmid DNA. *J Control Release* 2001; 77: 345–355.
54. Rivolta I, Panariti A, Lettiero B, et al. Cellular uptake of coumarin-6 as a model drug loaded in solid lipid nanoparticles. *J Physiol Pharmacol* 2011; 62: 45–53.
55. Arora S, Rajwade JM, and Paknikar KM. Nanotoxicology and in vitro studies: the need of the hour. *Toxicol Appl Pharmacol* 2012; 258: 151–165.
56. Elsaesser A and Howard CV. Toxicology of nanoparticles. *Adv Drug Deliv Rev* 2012; 64: 129–137.
57. Riley MR, Boesewetter DE, Turner RA, et al. Comparison of the sensitivity of three lung derived cell lines to metals from combustion derived particle matter. *Toxicol In Vitro* 2005; 19: 411–319.
58. Tavitian B, Marzabal S, Boutet V, et al. Characterization of a synthetic anionic vector for oligonucleotide delivery using in vivo whole body dynamic imaging. *Pharm Res* 2002; 19: 367–376.
59. Dou H, Grotepas CB, McMillan JM, et al. Macrophage delivery of nanoformulated antiretroviral drug to the brain in a murine model of neuroAIDS. *J Immunol* 2009; 183: 661–669.
60. Zhu M, Nie G, Meng H, et al. Physicochemical properties determine nanomaterial cellular uptake, transport and fate. *Acc Chem Res* 2013; 46: 622–631.
61. Doktorovova S, Souto EB, and Silva AM. Nanotoxicology applied to solid lipid nanoparticles and nanostructured lipid carriers-A systematic review of in vitro data. *Eur J Pharm Biopharm* 2014; 87: 1–18.
62. Pelchen-Matthews A, Kramer B, and Marsh M. Infectious HIV-1-assembles in late endosomes in primary macrophages. *J Cell Biol* 2003; 162:443–455.
63. Schmutz M, Durand D, Debin A, et al. DNA packing in stable lipid complexes designed for gene transfer imitates DNA compaction in bacteriophage. *Proc Natl Acad Sci USA* 1999; 96: 12293–12298.
64. Thierry AR, Norris V, Molina F, et al. Lipoplex nanostructures reveal a general self-organization of nucleic acids. *Biochem Biophys Acta* 2009; 1790: 385–394.
65. Chiu YL, Ali A, Chu CY, et al. Visualizing a correlation between siRNA localization, cellular uptake, and RNAi in living cells. *Chem Biol* 2004; 11: 1165e1175.
66. Berezna SY, Supekova L, Supek F, et al. siRNA in human cells selectively localizes to target RNA sites. *Proc Natl Acad Sci USA* 2006; 113: 7682e7687.
67. Lavigne C and Thierry AR. Specific subcellular localization of siRNAs delivered by lipoplex in MCF-7 breast cancer cells. *Biochimie* 2007; 89: 1245–1251.
68. Chen B, Xu W, Pan R, et al. Design and characterization of a new peptide vector for short interfering RNA delivery. *J Nanobiotechnology* 2015; 13: 39.
69. Kenny GD, Bienemann AS, Tagalakis AD, et al. Multifunctional receptor-targeted nanocomplexes for the delivery of therapeutic nucleic acids to the brain. *Biomaterials* 2013; 34: 9190–9200.
70. Tagalakis AD, Kenny GD, Bienemann AS, et al. PEGylation improves the receptor-mediated transfection efficiency of peptide-targeted, self-assembling, anionic nanocomplexes. *J Control Release* 2014; 174: 177–187.
71. Cho WS, Duffin R, Bradley M, et al. Predictive value of in vitro assays depends on the mechanism of toxicity of metal oxide nanoparticles. *Part Fibre Toxicol* 2013; 10: 55.
72. Gonçalves DM and Girard D. Zinc oxide nanoparticles delay human neutrophil apoptosis by a de novo protein synthesis-dependent and reactive oxygen species independent mechanism. *Toxicol In Vitro* 2014; 28: 926–931.
73. López-Rincón G, Pereira-Suárez AL, Del Toro-Arreola S, et al. Lipopolysaccharide induces the expression of an auto-crine prolactin loop enhancing inflammatory response in monocytes. *J Inflamm (Lond)* 2013; 10: 24.
74. Schildberger A, Rossmann E, Eichhorn T, et al. Monocytes, peripheral blood mononuclear cells, and THP-1 cells exhibit different cytokine expression patterns following stimulation with lipopolysaccharide. *Mediators Inflamm* 2013; 2013: 697972.
75. Simard JC, Vallieres F, de Liz R, et al. Silver nanoparticles induce degradation of the endoplasmic reticulum stress sensor activating transcription factor-6 leading to activation of the NLRP-3 inflammasome. *J Biol Chem* 2015; 290: 5926–5939.
76. Lavigne C, Yelle J, and Sauv e G. Lipid-based delivery of combinations of antisense oligodeoxynucleotides for the in vitro inhibition of HIV-1 replication. *AAPS PharmSci* 2001; 3(1): E7.